The Biochemistry of Methane Oxidation

Amanda S. Hakemian and Amy C. Rosenzweig

Departments of Biochemistry, Molecular Biology and Cell Biology and of Chemistry, Northwestern University, Evanston, Illinois 60208;
email: a-hakemian@northwestern.edu, amyr@northwestern.edu

Annu. Rev. Biochem. 2007. 76:223–41

First published online as a Review in Advance on February 28, 2007

The *Annual Review of Biochemistry* is online at biochem.annualreviews.org

This article's doi:
10.1146/annurev.biochem.76.061505.175355

0066-4154/07/0707-0223$20.00

Key Words

copper switch, methanobactin, methanotroph, particulate methane monooxygenase

Abstract

Methanotrophic bacteria oxidize methane to methanol in the first step of their metabolic pathway. Two forms of methane monooxygenase (MMO) enzymes catalyze this reaction: soluble MMO (sMMO) and membrane-bound or particulate MMO (pMMO). pMMO is expressed when copper is available, and its active site is believed to contain copper. Whereas sMMO is well characterized, most aspects of pMMO biochemistry remain unknown and somewhat controversial. This review emphasizes advances in the past two to three years related to pMMO and to copper uptake and copper-dependent regulation in methanotrophs. The pMMO metal centers have been characterized spectroscopically, and the first pMMO crystal structure has been determined. Significant effort has been devoted to improving in vitro pMMO activity. Proteins involved in sMMO regulation and additional copper-regulated proteins have been identified, and the *Methylococcus capsulatus* (Bath) genome has been sequenced. Finally, methanobactin (mb), a small copper chelator proposed to facilitate copper uptake, has been characterized.

Contents

INTRODUCTION

Methanotrophic bacteria utilize methane as their sole carbon and energy source (1). Found in a variety of habitats, including extreme environments (2), methanotrophs comprise 13 genera within the α and γ Proteobacteria (3). These organisms play an important role in the global carbon cycle and are potentially useful in curtailing the contribution of methane emissions to global warming (1, 4, 5). Oxidation of methane to methanol, the first step in methane metabolism, is catalyzed by methane monooxygenase (MMO) enzymes, which have attracted much attention for their possible applications in catalyst development (6) and/or bioremediation (7, 8). There are two forms of MMO, soluble MMO (sMMO) (9) and membrane-bound or particulate MMO (pMMO) (10). All but one genus of methanotrophic bacteria express pMMO, and a small subset produces both pMMO and sMMO (3). In this subset, differential expression of the two MMOs is controlled by the concentration of copper in the growth medium, with sMMO only produced at low copper concentrations (11–13). The mechanism of this "copper switch" is not known. Most studies of MMO have focused on enzymes from two organisms in this subset, *Methylococcus capsulatus* (Bath) and *Methylosinus trichosporium* OB3b.

sMMO comprises three components, a hydroxylase (MMOH), which houses the active site, a reductase (MMOR), which shuttles electrons from NADH to the active site of MMOH, and a regulatory protein (MMOB) that is required for activity (9). MMOH consists of three polypeptides arranged as an $\alpha_2\beta_2\gamma_2$ dimer (14). Methane and dioxygen bind at a carboxylate-bridged diiron center, similar to diiron centers found in the ribonucleotide reductase R2 protein (15), the stearoyl acyl-carrier protein Δ^9 desaturase (16), and a growing family of bacterial multicomponent monooxygenases (BMMs) that includes toluene monooxygenases, phenol hydroxylases, and alkene monooxygenases (17). A number of recent reviews have focused on structural (18), mechanistic (19), and evolutionary (17) aspects of sMMO and the BMM family. Because sMMO has a wide substrate specificity, oxidizing alkanes, alkenes, and aromatics (20), it has been a favored target for bioremediation applications (8). pMMO is more practical for in situ bioremediation for two reasons, however. First, only a few methanotrophs produce sMMO (3), and second, sMMO expression is repressed at the high levels of copper found in polluted environments (21).

Although pMMO is much more prevalent than sMMO in nature, less is known about

MMO: methane monooxygenase

sMMO: soluble methane monooxygenase

pMMO: particulate methane monooxygenase

its biochemistry, owing to difficulties working with an integral membrane protein. pMMO is composed of three subunits, α, β and γ, also known as pmoA, pmoB, and pmoC, respectively (10, 22). Ammonia monooxygenase (AMO), a pMMO homolog and the only enzyme other than sMMO and pMMO known to oxidize methane, has a similar polypeptide composition (23, 24). The metal content of pMMO has been controversial, but the active site is generally believed to contain copper ions (10, 25). pMMO has a more limited substrate specificity than sMMO (26), a property that could potentially be altered for bioremediation purposes once the active site has been characterized.

Whereas sMMO was the main focus in the field of methane oxidation biochemistry 10–20 years ago, interest in pMMO has been increasing over the past decade. This review focuses on recent advances in biological methane oxidation related to pMMO and to copper uptake and copper-dependent regulation in methanotrophs. Significant discoveries in the past two to three years include completion of the *M. capsulatus* (Bath) genome, identification and characterization of proteins involved in regulation of sMMO, detection of additional proteins that are copper regulated, more complete spectroscopic characterization of the pMMO metal centers, the first crystal structure of pMMO, improved activity for isolated pMMO, and detailed characterization of a novel copper chelator called methanobactin (mb). We highlight these advances, which were reported after the last comprehensive pMMO review (10), in the context of previous work with an emphasis on key unresolved issues.

GENETICS AND REGULATION

The genome of *M. capsulatus* (Bath) was completed and was the first methanotroph genome to become available. Proteins that may participate in the regulation of sMMO as well as additional copper-regulated genes have been identified recently.

The *M. capsulatus* (Bath) Genome

The *M. capsulatus* (Bath) genome comprises 3.3 megabases and includes 51 identifiable insertion elements and two putative prophages (27). As determined previously (28, 29), the genes encoding pMMO are present in multiple copies with two complete copies of the *pmoCAB* operon and a third copy of *pmoC*, *pmoC3*, located adjacent to three genes of unknown function. Mutants of *M. capsulatus* (Bath) in which one of the two copies of the *pmoCAB* operon is disrupted grow on methane, although they show decreased methane oxidation rates compared to wild-type bacteria. If both gene copies are disrupted, the cells are not viable, however. Interestingly, researchers were unable to isolate mutants in which *pmoC3* is disrupted, indicating this gene may play an essential role in methanotroph growth (29). Redundancy is also observed for other enzymes in the metabolic pathway, including methanol dehydrogenase and formate dehydrogenase. By contrast, the genes encoding sMMO occur only once. A transposase is present in some clones between the *mmoB* and *mmoZ* genes, which encode the regulatory protein B and the γ subunit of MMOH, respectively (30). Beyond the genes encoding enzymes in methane-dependent metabolism, genome analysis suggests the ability of methanotrophs to utilize sugars, oxidize chemolithotrophic hydrogen and sulfur, and exist under conditions of low oxygen tension (27). This proposed metabolic flexibility is not necessarily consistent with known methanotroph physiology and requires further study (31).

Copper trafficking proteins encoded by the genome may be of importance in the copper-regulated expression of the two MMOs or copper delivery to pMMO. Three homologs of the P_{1B}-type copper transporting ATPases are encoded (MCA0705, MCA0805, MCA2072) (32) as are homologs of soluble copper chaperones in the Atx1/CopZ (MCA0611) (33, 34) and PcoC/CopC (MCA0808, MCA2170) (35, 36) families.

mb: methanobactin

There is also a putative metal responsive transcription factor (MCA1339), annotated as a mercuric resistance operon regulatory protein. Finally, it should be noted that the genome encodes two putative nonribosomal peptide synthetases (MCA1883, MCA2107), which could be involved in the biosynthesis of the copper chelator mb (37) (*vide infra*).

Regulation of sMMO

In methanotrophs that express both forms of MMO, sMMO is expressed at <0.8 μM copper in the growth medium, whereas at ~4 μM copper, pMMO is expressed and extensive intracytoplasmic membranes develop (12, 13, 38). In *M. capsulatus* (Bath), the concentrations of the three pMMO polypeptides and of the *pmoA* transcript increase proportionally with copper levels in the medium, up to ~60 μM copper, after which a decrease in the amounts of pMMO is observed (38). Candidate regulatory proteins for pMMO expression have not yet been identified. Addition of copper to both *M. capsulatus* (Bath) and *M. trichosporium* OB3b leads to a decrease in sMMO mRNA (39, 40), consistent with the existence of a copper-binding repressor protein (11, 41). Copper-responsive transcriptional repressors or activators have not been identified, but some progress has been made toward understanding regulation of sMMO.

Four genes located immediately downstream (3′) of the *M. capsulatus* (Bath) sMMO operon, *mmoG*, *mmoQ*, *mmoS*, and *mmoR* (42), may be involved in regulation (**Figure 1*a***).

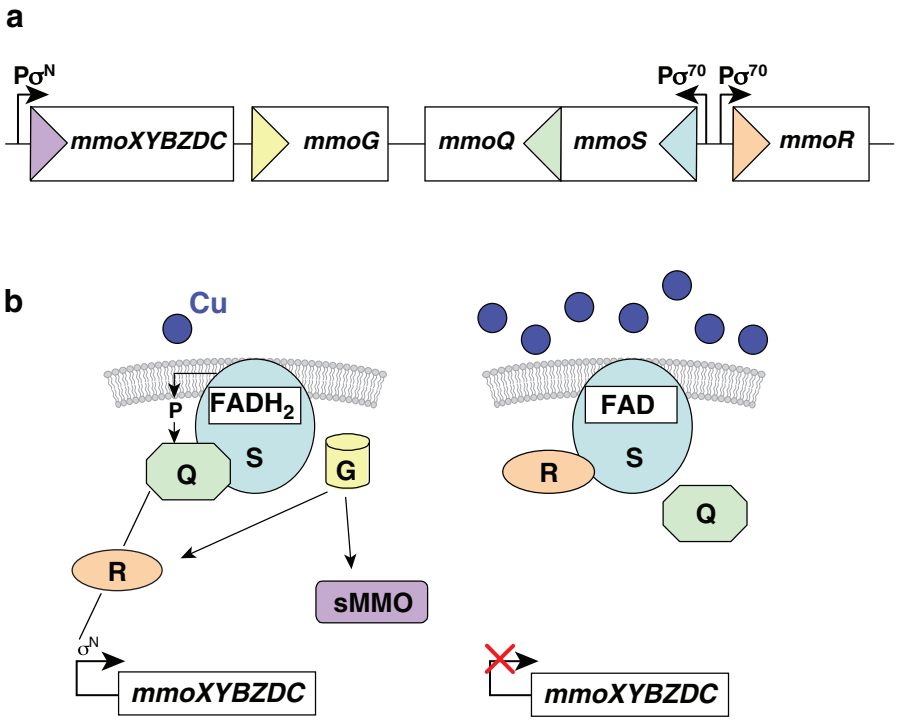

Figure 1

Regulation of sMMO. (*a*) In *M. capsulatus* (Bath), the regulatory genes *mmoG*, *mmoQ*, *mmoS*, and *mmoR* are found downstream of the *mmoXYBZDC* operon, which encodes the sMMO proteins. (*b*) Model for regulation of sMMO expression. (*left*) Low copper levels; (*right*) high copper levels. Abbreviations: FAD, flavin adenine dinucleotide; $FADH_2$, reduced flavin adenine dinucleotide; G, MmoG; Q, MmoQ; R, MmoR; S, MmoS; $P\sigma^N$, σ^N-dependent promoter; $P\sigma^{70}$, σ70-dependent promoter.

The *mmoG* and *mmoR* genes are also present in *M. trichosporium* OB3b, but are located upstream (5′) of the sMMO structural genes (43). According to the results of marker-exchange mutagenesis, both MmoG and MmoR are required for sMMO transcription. It should be noted that MmoR is not to be confused with MMOR, the reductase in the sMMO enzyme system. MmoG is predicted to be a GroEL homolog and may function in proper folding of MmoR or assembly of the sMMO complex (42, 43). MmoG might alternatively act as a coregulator together with MmoR, which is predicted to be a σ^N-dependent transcriptional activator that activates sMMO expression when copper levels are low (42). The MmoR sequence contains no obvious copper-binding motifs, however, suggesting that additional proteins might sense copper and transmit the signal to MmoR (42).

The proteins encoded by the *mmoQ* and *mmoS* genes could be involved in the copper-sensing mechanism. These proteins are homologous to two-component signaling systems in which a sensor protein detects an environmental stimulus, autophosphorylates a histidine residue within its histidine kinase domain, and then transfers the phosphoryl group to an aspartic acid residue in the response regulator protein, activating an effector domain (44, 45). MmoS resembles the sensor protein, and MmoQ corresponds to the regulator. The N-terminal sensing region of MmoS includes two predicted PAS-PAC domains. Because PAS-PAC domains detect changes in redox potential, light, or concentrations of small ligands (46, 47), MmoS is a reasonable candidate for participating in the copper switch, either directly or indirectly (42). MmoS lacking the N-terminal transmembrane domain has been characterized biochemically (48). Purified MmoS is a 480-kDa tetramer containing one flavin adenine dinucleotide (FAD) cofactor per monomer that is localized in the PAS-PAC domains. No evidence for copper binding has been obtained, indicating that MmoS does not sense copper directly. The properties of MmoS, including a redox potential of MmoS-bound FAD of –290 ± 2 mV at pH 8.0 and 25°C, are quite similar to those of the sensor protein, NifL, from diazotrophic bacteria. NifL senses oxygen or fixed nitrogen via an FAD cofactor and subsequently inhibits the ability of the NifA protein to activate transcription of genes involved in nitrogenase biosynthesis (49).

Several models have been proposed for sMMO regulation by these proteins. In *M. trichosporium* OB3b, MmoR is proposed to be inactivated by a copper signal, either directly or through MmoG. The inactive MmoR then cannot activate transcription of the sMMO genes (43). In *M. capsulatus* (Bath), an unknown copper sensor is proposed to transmit a signal to MmoS, which transfers a phosphoryl group to MmoQ. MmoQ then regulates sMMO expression via an interaction with MmoR (42). A more detailed variation of this model takes into account the possible redox-sensing ability of the FAD cofactor in MmoS (48) (**Figure 1*b***). In this third scenario, the MmoS FAD cofactor is present at low copper levels as reduced flavin adenine dinucleotide ($FADH_2$). This form of MmoS phosphorylates MmoQ, which interacts with MmoR and promotes MmoS transcription. At higher copper levels, $FADH_2$ is oxidized to FAD, causing a conformational change in MmoS that allows it to interact directly with MmoR, preventing MmoR from activating transcription. It is unclear exactly how copper concentrations might change the redox state of the FAD cofactor. The latter two models remain subject to the caveat that it has not yet been demonstrated that MmoS and/or MmoQ are essential for copper-dependent sMMO regulation. In addition, no evidence for the protein-protein interactions invoked in these models has been reported.

Additional Copper-Regulated Genes

In addition to the two MMOs, multiple other proteins are differentially expressed as a function of copper concentrations in the

growth medium. Several of these proteins were identified using sodium dodecyl sulfate-polyacrylamide gel electrophoresis and N-terminal sequencing prior to completion of the *M. capsulatus* (Bath) genome. In *M. capsulatus* (Bath), at least two formaldehyde dehydrogenases (FalDH) are regulated by copper, with a dye-linked FalDH expressed in the presence of copper and an $NAD(P)^+$-linked FalDH expressed under low-copper conditions (50). The copper-dependent expression of the different FalDHs is consistent with the way each MMO may be linked to the electron transport chain. The $NAD(P)^+$-linked FalDH is expressed under the same conditions as sMMO, which couples to the electron transport chain through NADH. The dye-linked FalDH, expressed with pMMO, is coupled to the electron transport chain through the cytochrome bc_1 complex, consistent with electron flow from the cytochrome bc_1 complex to pMMO (22).

Proteins of unknown function repressed by copper include CorA, an ~28.5-kDa membrane-bound protein from *Methylomicrobium albus* BG8 (51), and MopE, a cell surface-associated protein from *M. capsulatus* (Bath) (52, 53). Deletion of CorA affects cell growth, which cannot be rescued by copper addition (51). MopE exists in two forms, a 66-kDa cell surface-associated protein ($MopE^C$) and a 46-kDa protein, comprising the C-terminal part of $MopE^C$, which is secreted from the bacteria into the growth media ($MopE^*$). Both $MopE^C$ and $MopE^*$ are copper repressible (53), and $MopE^*$ is similar in sequence to *M. albus* BG8 CorA (52). Both proteins may play a role in copper uptake (51, 53), but neither sequence contains obvious copper-binding motifs. Additional biochemical and genetic studies are required to define the functions of MopE and CorA.

Immediately upstream of *mopE* in the *M. capsulatus* (Bath) genome is another copper-repressible gene (*MCA2590*), which encodes a protein homologous to the bacterial diheme cytochrome *c* peroxidase (BCCP) family (54). Unlike other members of the BCCP family, this protein is localized to the external surface of the outer membrane, rather than the periplasm. The sequence contains two heme-binding motifs, and *c*-type heme has been detected. Interestingly, an unannotated ORF in *M. albus* BG8, found immediately downstream of the gene encoding CorA, is 50% identical to the N terminus of this heme protein (54). The physiological role of the *MCA2590* gene product has not been determined, although it has been suggested, based on the proximity of the genes and their similar expression profile, that its function is linked with that of MopE (54).

The effects of copper concentration on protein expression in *M. capsulatus* (Bath) have also been investigated by a proteomics approach using cleavable isotope-coded affinity technology (55). This study was conducted while the genome sequencing was in progress. Of 682 proteins identified, 60 were upregulated and 68 were downregulated by copper. Most of the proteins exhibiting differential expression were biosynthetic enzymes. Notably, a hemerythrin, also identified independently by two-dimensional gel electrophoresis (56), was expressed at high copper levels. Hemerythrins are oxygen carriers found in marine invertebrates and are characterized by a dinuclear iron center housed within a four-helix bundle. Sequence analysis, combined with spectroscopic characterization of the purified protein, indicates that the *M. capsulatus* (Bath) hemerythrin is the first example of a prokaryotic hemerythrin. On the basis of these data, it probably binds oxygen, and a role in providing oxygen specifically to pMMO has been postulated (55, 56).

OVERALL STRUCTURE OF pMMO

Structural characterization of pMMO has been challenging due to the difficulty of working with an integral membrane protein. In this section, structural insights provided by the 2.8-Å resolution crystal structure and the 23-Å resolution cryoelectron microscopy

structure, both published in 2005, are discussed.

The 2.8-Å Resolution Crystal Structure

The crystal structure of pMMO from *M. capsulatus* (Bath) has been determined to 2.8-Å resolution (57–59). pMMO is a trimer, approximately 105 Å long and 90 Å in diameter, composed of three copies of each subunit in an $\alpha_3\beta_3\gamma_3$ polypeptide arrangement (**Figures 2** and **3**). The soluble region, which extends ~45 Å from the membrane, is composed of six cupredoxin-like β-barrels, two from each copy of the pmoB subunit. Each pmoB subunit also contains two transmembrane helices, which together with seven helices from each pmoA subunit and five from each pmoC subunit add up to a total of 42 transmembrane helices. Each αβγ protomer houses three metal centers (*vide infra*). There is an opening at the center of the pMMO trimer, ~11 Å wide in the soluble region and ~22 Å within the membrane (**Figure 3*a***). In the soluble region, this central cavity is lined with charged residues and likely contains solvent, although no water molecules could be modeled at 2.8-Å

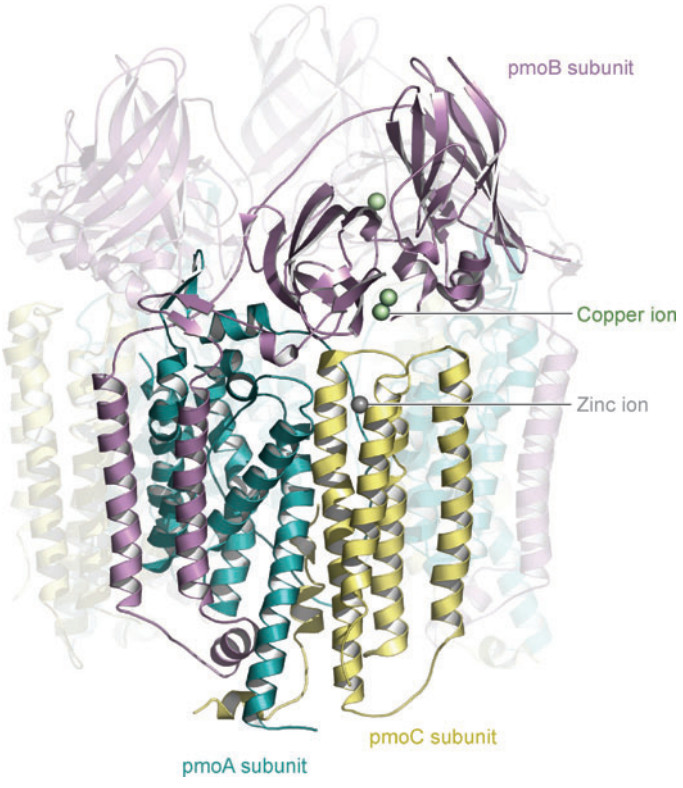

Figure 2

The pMMO trimer [Protein Data Bank (PDB) accession code 1YEW] with one protomer highlighted.

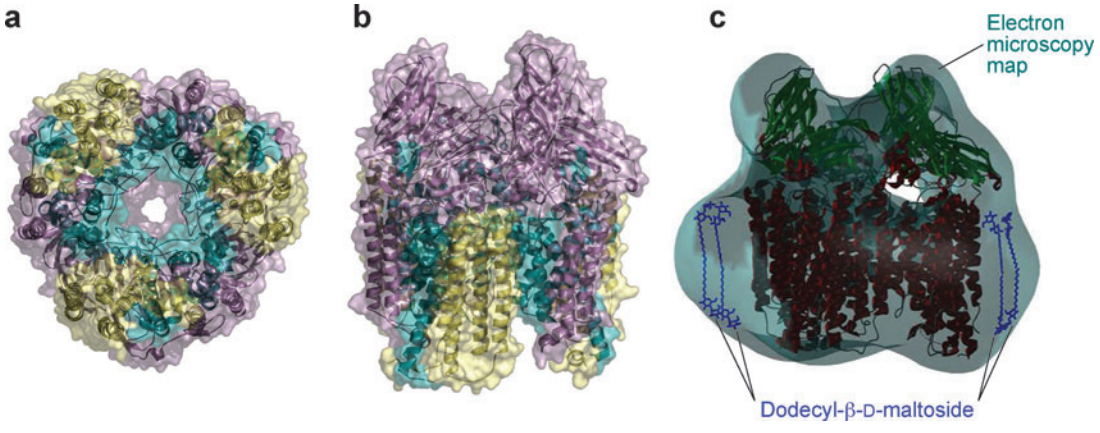

Figure 3

Surface representations of pMMO viewed (*a*) perpendicular to and (*b*) parallel to the membrane normal and (*c*) the pMMO crystallographic coordinates and four molecules of dodecyl-β-D-maltoside (extracted from PDB entry 1qla) docked into the electron microscopy map.

EM: electron microscopy

EPR: electron paramagnetic resonance

resolution. In the transmembrane region, this opening is lined with hydrophobic residues and is probably occupied by disordered detergent molecules, also not discernible in the crystal structure. The $\alpha_3\beta_3\gamma_3$ trimeric structure was unexpected because prior biochemical studies suggested either a monomeric $\alpha\beta\gamma$ (60) or a dimeric $\alpha_2\beta_2\gamma_2$ (61) arrangement (10).

Cryoelectron Microscopy Structure

Electron microscopy (EM) has also been used to determine the pMMO structure. Early electron micrographs of pMMO from *M. capsulatus* (strain M) revealed particles with a hexagonal shape, approximately 9 nm in diameter (62). Each particle had six maxima of protein density, interpreted to indicate a hexameric structure (62). In light of the crystal structure, it is probable that these six maxima correspond to the six β-barrels in the soluble region of pMMO. More recent electron micrographs of catalytically active pMMO-containing membranes reveal a threefold symmetry (63). Moreover, a 23-Å resolution structure of *M. capsulatus* (Bath) pMMO determined by EM and single-particle analysis reveals a complex consistent in size and shape with the crystallographic model (63) (**Figure 3*c***). Taken together, these EM data strongly suggest that the trimeric arrangement observed in the crystal structure is physiologically relevant. The EM structure includes several features not observed in the crystal structure (63) (**Figure 3*c***). First, there is a "belt" of density around the transmembrane region that is interpreted as a ring of detergent molecules, specifically dodecyl-β-D-maltoside, which was used to prepare the samples. Electron density attributed to detergent also fills the central opening at the transmembrane end of pMMO. Second, there are regions of low density or "holes" in the soluble domains. These regions together with the central opening may represent sites of substrate entry or product egress.

THE pMMO METAL CENTERS

Many laboratories have investigated the metal centers in pMMO by spectroscopic methods. In this section, these results are summarized in the context of the metal centers observed in the *M. capsulatus* (Bath) pMMO crystal structure.

Metal Content

Although it is generally accepted that pMMO is a metalloenzyme, the nature of the metal center(s) has been the subject of much debate. All researchers find copper associated with pMMO, but a wide range of stoichiometries has been reported and has been tabulated previously (10). In brief, copper contents for membrane-bound pMMO range from 4–59 copper ions per 100 kDa. For purified *M. capsulatus* (Bath) pMMO, four different laboratories report varied stoichiometries: 2 copper ions (64), 2–3 copper ions (61), 8–10 copper ions (38), and 15–20 copper ions (60, 65). The first three values can be considered similar because the 8–10 copper ions include 6–8 molecules of mb (*vide infra*), which are not present in the first two preparations, and 2 copper ions per 100 kDa pMMO. Consistent with this stoichiometry for the *M. capsulatus* (Bath) enzyme, purified pMMO from *M. trichosporium* OB3b contains 2 copper ions per 100 kDa (66). The origin of the higher values reported by Chan and coworkers remains unclear. In addition to copper, iron is found in some, but not all (60), preparations of both membrane-bound and purified pMMO. The reported stoichiometries are 0.75–2.5 iron ions per 100 kDa purified *M. capsulatus* (Bath) pMMO (22, 38, 61, 64).

Spectroscopic Studies

The pMMO copper centers in both membrane-bound and purified *M. capsulatus* (Bath) pMMO have been studied extensively by electron paramagnetic resonance (EPR) spectroscopy. On the basis of the hyperfine

splitting pattern of a broad isotropic signal at $g \sim 2.1$, Chan and coworkers (67) have proposed the presence of a ferromagnetically coupled trinuclear Cu(II) cluster. They also observed a type 2 Cu(II) signal, assigned to a second trinuclear cluster in which two of the three Cu(II) ions are antiferromagnetically coupled (68). By contrast, researchers in four other laboratories have observed only the type 2 signal using a variety of samples from three different organisms (22, 38, 61, 64, 69). This type 2 signal is not attributed to a trinuclear cluster and accounts for 40%–50% of the total copper present (61, 64). Alternative assignments for the signal interpreted as a trinuclear cluster include mb (22), superposition of a radical signal with that from the type 2 center (70), $CuFe(CN)_6^{2-}$ (71), or adventitiously bound copper ions (64).

X-ray absorption spectroscopic (XAS) data also provide insight into the pMMO metal centers (61, 72). The X-ray absorption near edge spectra (XANES) of as-isolated samples, containing 2–3 copper ions per 100 kDa, demonstrate that the copper centers can undergo redox chemistry. A feature at 8984 eV, attributable to a Cu(I) 1s→4p transition, increases in intensity upon chemical reduction with dithionite, indicating that some, but not all, of the copper ions are present as Cu(I) in purified pMMO. Treatment with H_2O_2 diminishes this peak, suggesting that some oxidation can occur, although complete oxidation has not been achieved. Extended X-ray absorption fine structure (EXAFS) data are best fit with two shells of backscatterers. The first shell is best fit with two Cu-O/N ligand environments with Cu-O/N distances ranging from 1.93 to 2.22 Å, depending on the sample and oxidation state. A second scattering interaction, observed in all samples, is best fit with a Cu-Cu interaction at 2.51 Å for as-isolated and oxidized pMMO and 2.65 Å for reduced pMMO. These data are the only direct spectroscopic evidence of a multinuclear copper cluster. The possibility of a Cu-Fe center with a short metal-metal distance was ruled out by Fe XAS data, which indicate the presence of Fe(III), but with no Fe-metal scattering in the 2.5–2.65 Å range. The Fe EXAFS parameters, combined with the optical spectrum of purified pMMO (61) and the observation of an EPR signal characteristic of high-spin heme (72), suggest that the iron is due to heme contaminants. Heme is not observed in some iron-containing preparations, however (38), leaving the possibility of a functional iron center.

XANES: X-ray absorption near edge structure

EXAFS: extended X-ray absorption fine structure

XAS: X-ray absorption spectroscopy

Crystallographic Data

Three metal centers were found in the crystal structure of *M. capsulatus* (Bath) pMMO (57, 58) (**Figure 4**). A dinuclear copper

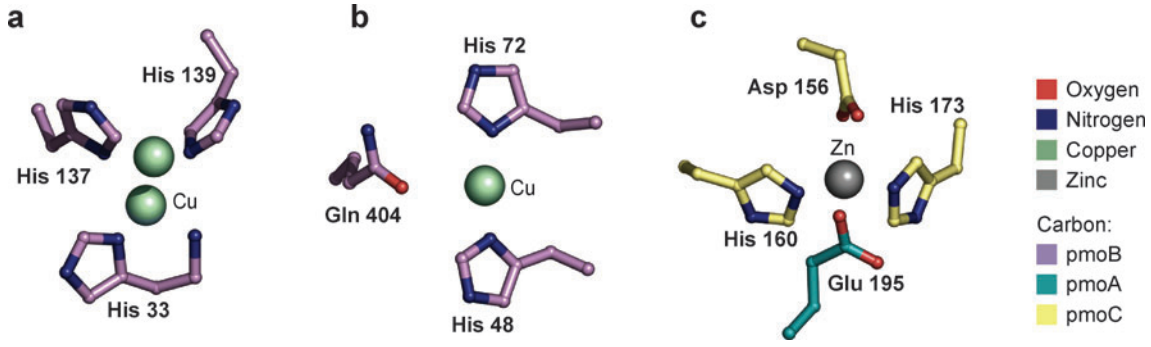

Figure 4

The dicopper (*a*), monocopper (*b*), and zinc (*c*) sites modeled in the pMMO crystal structure. Data reported in Reference 57.

center is located in the N-terminal β-barrel of the pmoB subunit ~10 Å above the membrane interface. The copper ions are coordinated by His 33, His 137, and His 139 (**Figure 4*a***). Notably, His 33 is the N-terminal residue of pmoB and ligates one of the copper ions through both its side chain δ nitrogen and the N-terminal amino nitrogen. The two copper ions are separated by ~2.6 Å, similar to the Cu-Cu distance obtained from EXAFS. The three histidine ligands are strictly conserved in pmoB and the related amoB subunit of AMO (**Figures 5** and **6*a***), consistent with an important role for this metal center. Two second-sphere ligands, Glu 35 and Gly 152, which are hydrogen bonded to the coordinating histidines, are also highly conserved.

A mononuclear copper center is also found in the soluble region of pmoB, ~25 Å above the membrane. The copper ion is coordinated by the δ nitrogens of His 48 and His 72 (**Figure 4*b***). Residue His 48 is not conserved (**Figures 5** and **6*a***). In many methanotrophs, an asparagine residue is found at this position, and in most AMOs, the histidine is replaced with a glutamine. The second ligand, His 72, is conserved among most pmoB and amoB sequences, but in a few species of nitrifying bacteria, the corresponding residue is an arginine. An adjacent glutamine, Gln 404, which was proposed to hydrogen bond to solvent ligands not observed in the crystal structure (58), is not conserved at all (**Figure 5**). At 2.8 Å resolution, exogenous ligands were not detected at either copper center, but the EXAFS data indicate a coordination number of 2–4 for the O/N ligands, which is more than the two ligands to each copper ion in the crystal structure (72). The oxidation states of the copper ions present in the crystal structure are not known, but multiple scenarios have been considered. The scheme most consistent with the spectroscopic data is that the mononuclear site is Cu(I) and the dinuclear site is a completely localized, mixed valence Cu(I)Cu(II) site (72).

A third metal center, occupied in the structure by zinc from the crystallization buffer, is located within the membrane. A single zinc ion is coordinated by Asp 156, His 160, and His 173 from the pmoC subunit and Glu 195 from the pmoA subunit (**Figure 4*c***). All four of these residues are strictly conserved, strongly suggesting that this site is functionally important (**Figures 5** and **6*b***). Because purified pMMO contains less than 0.2 zinc ions per monomer (57), this site may be occupied by copper or iron in vivo. One possibility is a carboxylate-bridged diiron center, like that found in the active site of MMOH, but no spectroscopic evidence for such a center has been obtained.

Although the spectroscopic and crystallographic data have provided much information on the pMMO metal centers, their functions remain unclear, and the active site has not yet been identified. On the basis of sequence alignments, the mononuclear copper center seems unlikely to play an essential role. The dinuclear copper site is an attractive candidate for the active site because the residues are strictly conserved and because there is an adjacent hydrophobic pocket (57). Other dinuclear copper centers, such as that in tyrosinase (73), are capable of hydroxylation chemistry, but these sites have longer Cu-Cu distances and six rather than three coordinating histidine residues (74). The zinc center is also a reasonable option, depending on what metal ion or ions occupy this site in vivo. A third possibility is that the active site is metal depleted in the crystal structure. There is one region of hydrophilic residues within the membrane ~13 Å from the zinc site, composed of strictly conserved His 38, Met 42, Asp 47, Asp 49, and Glu 100 from pmoA and Glu 154 from pmoC (**Figure 6*b***). It is conceivable that a metal-binding site could be assembled by some combination of these residues.

pMMO AND CATALYSIS

The conditions necessary for the isolation of catalytically active pMMO have been researched extensively, but remain unclear. In this section, progress toward understanding

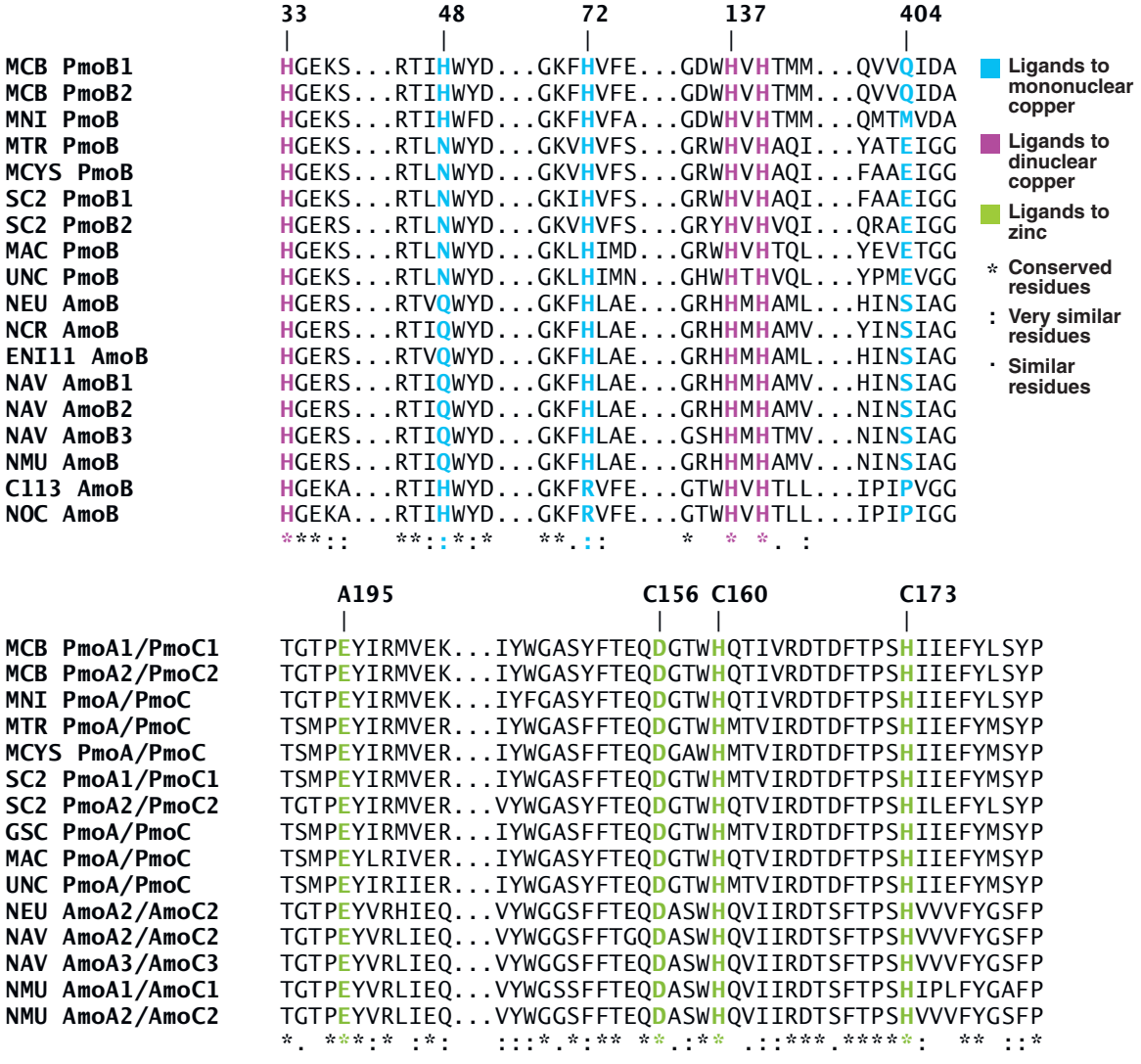

Figure 5

Multiple sequence alignments of pMMO and AMO subunits showing the ligands to the metal centers in the *M. capsulatus* (Bath) pMMO structure. Numbers above the alignment correspond to copy 2 of pMMO in *M. capsulatus* (Bath). Abbreviations: MCB, *M. capsulatus* (Bath); MNI, *Methylomicrobium* sp. NI; MTR, *M. trichosporium* OB3b; MCYS, *Methylocystis* sp. M; SC2, *Methylocystis* sp. SC2; MAC, *Methylocapsa acidiphila*; UNC, uncultured methanotroph; NEU, *Nitrosomonas europaea*; NCR, *Nitrosomonas cryotolerans*; ENI11, *Nitrosomonas* sp. ENI-11; NAV, *Nitrosospira* sp. NpAV; NMU, *Nitrosospira multiformis* ATCC 25196; C113, *Nitrosococcus* sp. C-113; NOC, *Nitrosococcus oceani*; GSC, *Methylocystis* sp. GSC357. GenBank accession numbers and alignments of the full subunit sequences are available online. See the **Supplemental Material link** in the online version of this chapter or at **http://www.annualreviews.org/**

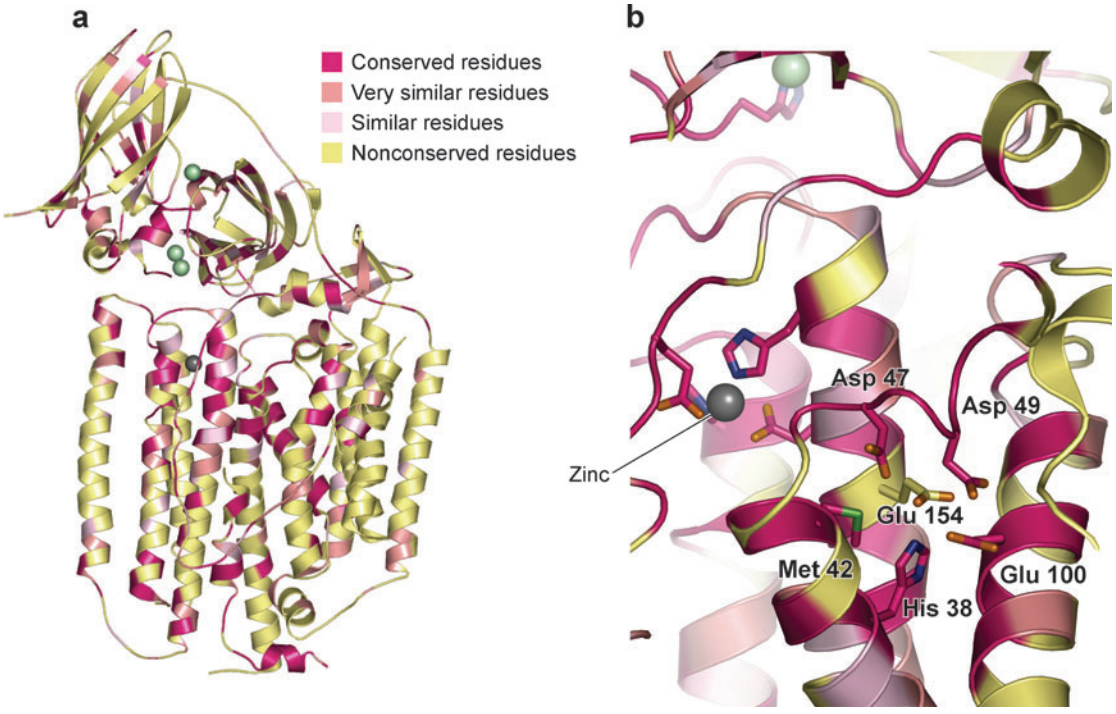

Figure 6

Multiple sequence alignments mapped to the pMMO crystal structure. (*a*) The pMMO protomer with conserved residues, very similar residues, and similar residues shown. (*b*) A conserved patch of hydrophilic residues adjacent to the zinc center that may represent an additional metal-binding site.

the catalytic activity and mechanism of pMMO is summarized.

Isolation and Activity

pMMO can oxidize alkanes and alkenes up to five carbons in length, but unlike sMMO, it cannot oxidize cyclic or aromatic hydrocarbons (8, 26). Obtaining purified pMMO that retains activity has been a significant issue in the field. Using the propylene oxidation assay (20) with either NADH or duroquinol (75) as a reductant, specific activities for *M. capsulatus* (Bath) pMMO of ~10–200 nmol (nanomole) propylene oxide (mg protein · min)$^{-1}$ for the membrane-bound enzyme and 2–126 nmol propylene oxide (mg protein · min)$^{-1}$ for purified preparations have been reported (22, 38, 61, 64, 65, 76, 77). For purified *M. trichosporium* OB3b pMMO, a specific activity of ~3–4 nmol propylene oxide (mg protein · min)$^{-1}$ has been reported (66). These values were obtained using a variety of purification procedures, which have been described in detail previously (10). A comparison of the different protocols suggests that several factors influence pMMO activity.

First, the concentration of copper in the growth medium is important. Addition of excess copper beyond that needed to switch from sMMO to pMMO expression increases the activity of pMMO in cell-free extracts, with reports of optimal concentrations ranging from 30 to 80 μM (12, 22, 38, 60). In addition, continuous addition of copper to the culture improves activity in purified pMMO (38), as does the use of fast-growing cells with doubling times <5 hr (64). Some iron in the growth medium is also necessary to obtain reasonable activity (38). Second,

anaerobicity might have an effect. The highest reported specific activity for membrane-bound pMMO, 290 nmol propylene oxide (mg protein · min)$^{-1}$, was obtained for pMMO isolated under anaerobic conditions (38), but another report indicated that anaerobic purification resulted in little to no activity (64). Third, activity is dependent on the solubilization procedure. All reported pMMO solubilization protocols employ dodecyl-β-D-maltoside, but different amounts are used. DiSpirito and coworkers (38) determined that the optimal detergent/protein ratio (w/w) is 1–1.25 mg dodecyl-β-D-maltoside per mg protein and observed a loss of the metal ions at nonoptimal detergent concentrations. Furthermore, increasing the detergent concentration in purified pMMO after solubilization resulted in inactivation (38). Because each laboratory purifying pMMO handles these variables in a different fashion (10), the discrepancies in activity and metal content are not surprising.

Physiological Reductant

The issue of pMMO activity is further complicated because the physiological reductant of pMMO is not known. It may be that disruption of the electron transport chain during purification contributes to problems maintaining pMMO activity (78). For membrane-bound pMMO, NADH can serve as a reductant for in vitro activity assays. Once pMMO is solubilized, however, only quinols produce activity (22, 61, 64), with duroquinol yielding the best results (75). Improved specific activities for pMMO have been obtained either by adding another protein back to purified pMMO or by partially purifying a pMMO sample that contains additional proteins. For example, addition of purified type 2 NADH:quinone oxidoreductase (NDH-2) together with NADH and duroquinol increased specific activity in purified pMMO samples by up to 35% (38). Alternatively, Dalton and coworkers (64) reported that copurification with two polypeptides of molecular masses 63 and 8 kDa was necessary to obtain activity with duroquinol. No activity was observed in the absence of these proteins, and reconstitution of the complex gave only 10% of the original activity. The 63-kDa component is likely methanol dehydrogenase (64).

These observations have led to several proposals for the electron transfer pathway. In one scenario, NDH-2 uses NADH generated by oxidation of formate and formaldehyde to reduce endogenous quinones, which then reduce pMMO either directly or through an additional reductase. This model is consistent with the observation that the NDH-2 inhibitor diphenyliodonium inhibits NADH-dependent membrane-bound pMMO activity (78). The activity observed in the presence of the putative 63-kDa methanol dehydrogenase suggests a role for methanol dehydrogenase in electron transfer, but neither methanol nor formaldehyde enhanced activity, perhaps owing to loss of a cytochrome component (64). Finally, the cytochrome bc_1 complex may donate electrons to pMMO, perhaps through ubiquinone 8. This model is consistent with the coexpression of pMMO and the dye-linked FalDH (50). It is not known whether any of these proteins interact directly with pMMO in vivo. Interestingly, the crystal structure reveals a negatively charged patch on the pMMO surface, which could represent a docking site for a partner reductase (57).

Mechanistic Studies

Some attempts have been made to address the pMMO chemical mechanism using membrane preparations. Experiments with chiral alkanes, which have provided insight into the sMMO mechanism (19), suggest a concerted mechanism, rather than the involvement of radical or cation intermediates (77, 79). No carbon kinetic isotope effect was observed for propane oxidation, which was interpreted as indicating little or no structural change at the carbon center during transition state formation in the rate-limiting step (80). When

Cu-mb: copper-bound methanobactin

oxidizing multicarbon compounds, pMMO was shown to oxidize the C-2 position preferentially (81). On the basis of these limited studies, Chan and coworkers (77) have proposed that the C-H bond of the substrate is presented to a "hot" oxygen species, resulting in the formation of a nonlinear C···O···H transition state. Using density functional theory calculations on model complexes, they have further argued that a trinuclear bis(μ_3-oxo)Cu(II, II, III) center is best suited to this chemistry (82). Considering the absence of such a cluster in the crystal structure, the fact that these mechanistic studies were carried out on membrane preparations, and the discrepancy in metal ion content and activity among various pMMO preparations, these conclusions remain speculative. A more detailed discussion of possible mechanisms and active site locations can be found in Reference 83.

COPPER UPTAKE AND METHANOBACTIN

Because of the importance of copper in both the regulation and chemistry of pMMO, it is likely that methanotrophs possess a specialized copper acquisition system. Methanobactin (mb), a copper-chelating, siderophore-like molecule, is believed to play an important role in this uptake system, as well as possibly contributing to pMMO activity.

Methanobactin Structure and Properties

Initial evidence for a copper uptake system in methanotrophs was derived from studies of *M. trichosporium* OB3b mutants that constitutively express sMMO and do not express active pMMO or produce intracytoplasmic membranes. The extracellular media from these mutants also have an unusually high concentration of copper (21, 84). According to the prevailing hypothesis, this phenotype results from a defect in a copper-complexing agent, reminiscent of an iron siderophore (84). Candidate molecules for this copper chelator were later detected in the spent media of *M. trichosporium* OB3b (85, 86) and *M. capsulatus* (Bath) (22) grown at low copper concentrations. These compounds, referred to as copper-binding compounds or ligands, range in molecular mass from 382 to 1217 Da and bind a single copper ion with high affinity. Further characterization was hindered, however, by degradation and difficulties determining the sequence and chemical composition. These issues were resolved recently, and the crystal structure of the *M. trichosporium* OB3b copper-binding compound was determined. This molecule, renamed methanobactin (mb), has a molecular weight of 1217 Da and the sequence *N*-2-isopropylester-(4-thionyl-5-hydroxyimidazolate)-Gly^1-Ser^2-Cys^3-Tyr^4-pyrrolidine-(4-hydroxy-5-thionylimidazolate)-Ser^5-Cys^6-Met^7 (37, 87). The crystal structure reveals a pyramid-like structure, with a single copper ion coordinated by an N_2S_2 donor set at the base of the pyramid (37) (**Figure 7**).

The oxidation state of the chelated copper ion in mb was suggested to be Cu(I) on the basis of X-ray photoelectron spectroscopy and was confirmed by XAS and EPR analysis. The XANES spectrum of *M. trichosporium* OB3b copper-bound mb (Cu-mb) exhibits a 1s→4p transition at 8985 eV indicative of Cu(I) and lacks features attributable to Cu(II) (88). The EPR spectrum of Cu-mb only shows weak signals with $g_{||}$ and $A_{||}$ values that are characteristic of copper with N_xO_{4-x} ligands, as would be expected from adventitiously bound Cu(II) (22, 85, 88). Furthermore, EPR signals attributable to Cu(II) with sulfur ligation typically disappear <10 min after Cu(II) addition to mb (89). Thus, mb itself is capable of reducing Cu(II) to Cu(I). The optical spectrum of Cu-mb also lacks features characteristic of Cu(II) (87). Spectral and kinetic data suggest that mb initially binds Cu(II) as a dimer with coordination by 4-hydroxy-5-thionylimidazolate and possibly tyrosine, followed by reduction to Cu(I) and coordination by 4-thionyl-5-hydroxyimidazolate (90).

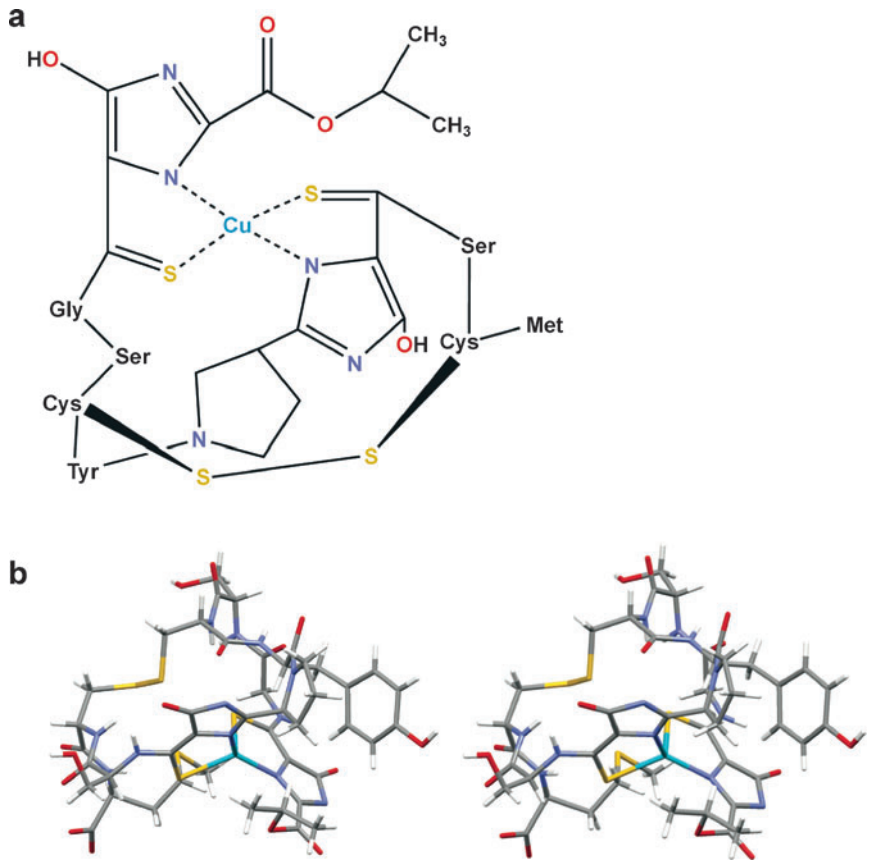

Figure 7

Methanobactin structure [Cambridge Crystallographic Data Center (CCDC) deposition number CCDC 241254] shown (*a*) schematically and (*b*) in stereo as a ball-and-stick representation. Data reported in Reference 37.

Possible Functions of Methanobactin

Several lines of evidence suggest that mb is involved in copper uptake. When *M. trichosporium* OB3b or *M. capsulatus* (Bath) cells are grown under copper-limited conditions, mb is present in the spent media. After copper supplementation, the level of mb in the medium decreases (22, 85, 86), and Cu-mb is found associated with the membranes (22, 85). The addition of stoichiometric quantities of mb and copper to the growth medium when *M. trichosporium* OB3B cells are switched from copper-starved to copper-rich conditions also decreases the lag time and stimulates growth (87).

Cu-mb is also proposed to play a role in pMMO activity. DiSpirito and coworkers have reported that an irreversible loss of pMMO activity occurs upon dissociation of Cu-mb from pMMO (22, 38, 89). Other preparations lacking Cu-mb do exhibit reasonable activity, however (63, 64, 66). In support of a role in activity, addition of *M. trichosporium* OB3b Cu-mb to *M. capsulatus* (Bath) cells expressing pMMO or to *M. capsulatus* (Bath) membrane fractions enhances activity. The specific activity of membrane-bound pMMO is increased by ~35% (89). Addition of Cu(II) alone also increases activity, but only by ~20%. These data should be considered with two caveats. First, Cu-mb and pMMO from two species were combined because procedures for isolating Cu-mb from *M. trichosporium* OB3b and pMMO from *M. capsulatus* (Bath) are best developed. It is not known whether mb has the same chemical composition in both organisms, however. Second, the effects of adding Cu(I) to the activity

assay were not reported. It may be that Cu-mb acts as a copper chaperone, increasing activity by delivering Cu(I) to the catalytic metal center.

The effect of Cu-mb on pMMO activity may be indirect. Cu-mb exhibits superoxide dismutase activity and thus may protect pMMO in cell-free extracts from oxidative damage (38). Alternatively, Cu-mb may interact with pMMO directly. This possibility has been probed by EPR spectroscopy (89). Addition of *M. trichosporium* OB3b Cu-mb to high activity membrane-bound *M. capsulatus* (Bath) pMMO resulted in an almost complete loss of the type 2 Cu(II) signal and the appearance of a free radical signal at $g = 2.005$. Addition of oxygen resulted in reappearance of the type 2 signal and an increase in intensity of the radical signal. Addition of methane and oxygen also resulted in reappearance of the type 2 signal, but the radical signal was no longer present. This radical signal disappeared upon purification (61), however, suggesting that it may not be relevant to pMMO. When these experiments were repeated on lower activity membrane preparations, the effects of Cu-mb were less pronounced. In some preparations, addition of Cu-mb resulted in the loss of the superhyperfine structure associated with the type 2 signal. Taken together, these EPR spectral changes were interpreted as evidence of an interaction between Cu-mb and the type 2 Cu(II) center of pMMO. Further studies using purified pMMO and Cu-mb from the same organism are clearly necessary.

SUMMARY POINTS

1. The genome of *M. capsulatus* (Bath) has been sequenced and offers the opportunity to investigate protein expression as a function of copper concentration.
2. The copper switch mechanism governing differential expression of sMMO and pMMO is not yet understood, but the sMMO regulatory proteins MmoR, MmoG, MmoS, and MmoQ may be involved.
3. Spectroscopic data indicate that pMMO contains a mixture of Cu(I) and Cu(II), of which some is present as a copper-containing cluster with a short Cu-Cu distance. Several pMMO preparations also contain iron.
4. The crystal structure of *M. capsulatus* (Bath) pMMO reveals a trimer, also observed by cryo-EM studies. A mononuclear copper center, a dinuclear copper center, and a mononuclear zinc site are present.
5. The specific activity of isolated pMMO is variable and depends on growth conditions as well as solubilization and purification protocols. The physiological reductant has not been identified.
6. Methanobactin, a 1217-Da Cu(I) chelator, likely functions in copper uptake and may also modulate pMMO activity.

FUTURE ISSUES

1. The specific factor(s) that sense copper and promote the switch from sMMO to pMMO expression need to be identified.
2. Additional crystal structures and spectroscopic data are required to establish the pMMO metal composition in vivo, the detailed coordination geometries of the metal centers, and, most importantly, the nature of the active site.

3. The in vivo function of methanobactin remains to be determined, and the biosynthetic enzymes and receptors involved in its handling should be investigated.
4. Once the pMMO active site is identified and high activity preparations of purified enzyme are obtained routinely, detailed mechanistic studies should be initiated.

ACKNOWLEDGMENTS

Work on pMMO in the laboratory of A.C.R. is supported by NIH GM070473. A.S.H. was supported in part by a National Science Foundation Graduate Research Fellowship. **Figure 3*c*** was kindly provided by Dr. A. Kitmotto (University of Manchester, United Kingdom).

LITERATURE CITED

1. Hanson RS, Hanson TE. 1996. *Microbiol. Rev.* 60:439–71
2. Trotsenko YA, Khmelenina VN. 2002. *Arch. Microbiol.* 177:123–31
3. Dumont MG, Murrell JC. 2005. *Methods Enzymol.* 397:413–27
4. Park S, Brown KW, Thomas JC. 2002. *Waste Manag. Res.* 20:434–44
5. Tol RSJ, Heintz RJ, Lammers PEM. 2003. *Clim. Change* 57:71–98
6. Periana RA, Bhalla G, Tenn WJ, Young KJH, Liu XY, et al. 2004. *J. Mol. Catal. A* 220:7–25
7. Lontoh S, Semrau JD. 1998. *Appl. Environ. Microbiol.* 64:1106–14
8. Sullivan JP, Dickinson D, Chase CA. 1998. *Crit. Rev. Microbiol.* 24:335–73
9. Merkx M, Kopp DA, Sazinsky MH, Blazyk JL, Müller J, Lippard SJ. 2001. *Angew. Chem. Int. Ed. Engl.* 40:2782–807
10. Lieberman RL, Rosenzweig AC. 2004. *Crit. Rev. Biochem. Mol. Biol.* 39:147–64
11. Murrell JC, McDonald IR, Gilbert B. 2000. *Trends Microbiol.* 8:221–25
12. Prior SD, Dalton H. 1985. *J. Gen. Microbiol.* 131:155–63
13. Stanley SH, Prior SD, Leak DJ, Dalton H. 1983. *Biotechnol. Lett.* 5:487–92
14. Rosenzweig AC, Frederick CA, Lippard SJ, Nordlund P. 1993. *Nature* 366:537–43
15. Nordlund P, Reichard P. 2006. *Annu. Rev. Biochem.* 75:681–706
16. Fox BG, Lyle KS, Rogge CE. 2004. *Acc. Chem. Res.* 37:421–29
17. Notomista E, Lahm A, DiDonato A, Tramontano A. 2003. *J. Mol. Evol.* 56:435–45
18. Sazinsky MH, Lippard SJ. 2006. *Acc. Chem. Res.* 39:558–66
19. Baik MH, Newcomb M, Friesner RA, Lippard SJ. 2003. *Chem. Rev.* 103:2385–419
20. Colby J, Stirling DI, Dalton H. 1977. *Biochem. J.* 165:395–402
21. Phelps PA, Agarwal SK, Speitel GEJ, Georgiou G. 1992. *Appl. Environ. Microbiol.* 58:3701–8
22. Zahn JA, DiSpirito AA. 1996. *J. Bacteriol.* 178:1018–29
23. Arp DJ, Sayavedra-Soto LA, Hommes NG. 2002. *Arch. Microbiol.* 178:250–55
24. Holmes AJ, Costello A, Lidstrom ME, Murrell JC. 1995. *FEMS Microbiol. Lett.* 132:203–8
25. Chan SI, Chen KHC, Yu SSF, Chen CL, Kuo SSJ. 2004. *Biochemistry* 43:4421–30
26. Burrows KJ, Cornish A, Scott D, Higgins IJ. 1984. *J. Gen. Microbiol.* 130:327–33
27. Ward N, Larsen O, Sakwa J, Bruseth L, Khouri H, et al. 2004. *PLoS Biol.* 2:e303
28. Semrau JD, Chistoserdov A, Lebron J, Costello A, Davagnino J, et al. 1995. *J. Bacteriol.* 177:3071–79
29. Stolyar S, Costello AM, Peeples TL, Lidstrom ME. 1999. *Microbiology* 145:1235–44
30. Stainthorpe AC, Lees V, Salmond GPC, Dalton H, Murrell JC. 1990. *Gene* 91:27–34

31. Kelly DP, Anthony C, Murrell JC. 2005. *Trends Microbiol.* 13:195–98
32. Argüello JM. 2003. *J. Membr. Biol.* 195:93–108
33. Banci L, Rosato A. 2003. *Acc. Chem. Res.* 36:215–21
34. Rosenzweig AC. 2002. *Chem. Biol.* 9:673–77
35. Wernimont AK, Huffman DL, Finney LA, Demeler B, O'Halloran TV, Rosenzweig AC. 2003. *J. Biol. Inorg. Chem.* 8:185–94
36. Zhang L, Koay M, Mahert MJ, Xiao Z, Wedd AG. 2006. *J. Am. Chem. Soc.* 128:5834–50
37. Kim HJ, Graham DW, DiSpirito AA, Alterman MA, Galeva N, et al. 2004. *Science* 305:1612–15
38. Choi DW, Kunz RC, Boyd ES, Semrau JD, Antholine WE, et al. 2003. *J. Bacteriol.* 185:5755–64
39. Nielsen AK, Gerdes K, Degn H, Murrell JC. 1996. *Microbiology* 142:1289–96
40. Nielsen AK, Gerdes K, Murrell JC. 1997. *Mol. Microbiol.* 25:399–409
41. Murrell JC, Gilbert B, McDonald IR. 2000. *Arch. Microbiol.* 173:325–32
42. Csáki R, Bodrossy L, Klem J, Murrell JC, Kovács KL. 2003. *Microbiology* 149:1785–95
43. Stafford GP, Scanlan J, McDonald IR, Murrell JC. 2003. *Microbiology* 149:1771–84
44. Stock AM, Robinson VL, Goudreau PN. 2000. *Annu. Rev. Biochem.* 69:183–215
45. West AH, Stock AM. 2001. *Trends Biochem. Sci.* 26:369–76
46. Hefti M, Françoijs KJ, de Vries LC, Dixon R, Vervoort J. 2004. *Eur. J. Biochem.* 271:1198–208
47. Taylor BL, Rebbapragada A, Johnson MS. 2001. *Antioxid. Redox Signal.* 3:867–79
48. Ukaegbu UE, Henery S, Rosenzweig AC. 2006. *Biochemistry* 45:10191–98
49. Martinez-Argudo I, Little R, Shearer N, Johnson P, Dixon R. 2004. *J. Bacteriol.* 186:601–10
50. Zahn JA, Bergmann DJ, Boyd JM, Kunz RC, DiSpirito AA. 2001. *J. Bacteriol.* 183:6832–40
51. Berson O, Lidstrom ME. 1997. *FEMS Microbiol. Lett.* 148:169–74
52. Fjellbirkeland A, Kruger PG, Bemanian V, Høgh BT, Murrell JC, Jensen HB. 2001. *Arch. Microbiol.* 176:197–203
53. Karlsen OA, Berven FS, Stafford GP, Larsen Ø, Murrell JC, et al. 2003. *Appl. Environ. Microbiol.* 69:2386–88
54. Karlsen OA, Kindingstad L, Angelskår SM, Bruseth LJ, Straume D, et al. 2005. *FEBS J.* 272:6324–35
55. Kao WC, Chen YR, Yi EC, Lee H, Tian Q, et al. 2004. *J. Biol. Chem.* 279:51554–60
56. Karlsen OA, Ramsevik L, Bruseth LJ, Larsen Ø, Brenner A, et al. 2005. *FEBS J.* 272:2428–40
57. Lieberman RL, Rosenzweig AC. 2005. *Nature* 434:177–82
58. Lieberman RL, Rosenzweig AC. 2005. *Dalton Trans.* 21:3390–96
59. Sommerhalter M, Lieberman RL, Rosenzweig AC. 2005. *Inorg. Chem.* 44:770–78
60. Yu SSF, Chen KHC, Tseng MYH, Wang YS, Tseng CF, et al. 2003. *J. Bacteriol.* 185:5915–24
61. Lieberman RL, Shrestha DB, Doan PE, Hoffman BM, Stemmler TL, Rosenzweig AC. 2003. *Proc. Natl. Acad. Sci. USA* 100:3820–25
62. Tsuprun VL, Akent'eva NP, Tagunova IV, Orlova EV, Grigoryan AN, et al. 1987. *Dokl. Akad. Nauk SSSR* 292:490–93 (In Russian)
63. Kitmitto A, Myronova N, Basu P, Dalton H. 2005. *Biochemistry* 44:10954–65
64. Basu P, Katterle B, Andersson KK, Dalton H. 2003. *Biochem. J.* 369:417–27
65. Nguyen HH, Elliott SJ, Yip JH, Chan SI. 1998. *J. Biol. Chem.* 273:7957–66
66. Miyaji A, Kamachi T, Okura I. 2002. *Biotechnol. Lett.* 24:1883–87
67. Hung SC, Chen CL, Chen KHC, Yu SSF, Chan SI. 2004. *J. Chin. Chem. Soc.* 51:1229–44

68. Chen KHC, Chen CL, Tseng CF, Yu SSF, Ke SC, et al. 2004. *J. Chin. Chem. Soc.* 51:1081–98
69. Lemos SS, Collins MLP, Eaton SS, Eaton GR, Antholine WE. 2000. *Biophys. J.* 79:1085–94
70. Yuan H, Collins MLP, Antholine WE. 1997. *J. Am. Chem. Soc.* 119:5073–74
71. Yuan H, Collins MLP, Antholine WE. 1998. *J. Inorg. Biochem.* 72:179–85
72. Lieberman RL, Kondapalli KC, Shrestha DB, Hakemian AS, Smith SM, et al. 2006. *Inorg. Chem.* 45:8372–81
73. Matoba Y, Kumagai T, Yamamoto A, Yoshitsu H, Sugiyama M. 2006. *J. Biol. Chem.* 281:8981–90
74. Rosenzweig AC, Sazinsky MH. 2006. *Curr. Opin. Struct. Biol.* 16:729–35
75. Shiemke AK, Cook SA, Miley T, Singleton P. 1995. *Arch. Biochem. Biophys.* 321:421–28
76. Katterle B, Gvozdev RI, Abudu N, Ljones T, Andersson KK. 2002. *Biochem. J.* 363:677–86
77. Yu SSF, Wu LY, Chen KHC, Luo WI, Huang DS, Chan SI. 2003. *J. Biol. Chem.* 278:40658–69
78. Shiemke AK, Arp DJ, Soto-Sayvedra LA. 2004. *J. Bacteriol.* 186:928–37
79. Wilkinson B, Zhu M, Priestley ND, Nguyen HHT, Morimoto H, et al. 1996. *J. Am. Chem. Soc.* 118:921–22
80. Huang DS, Wu SH, Wang YS, Yu SS, Chan SI. 2002. *ChemBioChem* 3:760–65
81. Elliott SJ, Zhu M, Tso L, Nguyen HH, Yip JHK, Chan SI. 1997. *J. Am. Chem. Soc.* 119:9949–55
82. Chen PPY, Chan SI. 2006. *J. Inorg. Biochem.* 100:801–9
83. Balasubramanian R, Rosenzweig AC. 2007. *Acc. Chem. Res.* In press
84. Fitch MW, Graham DW, Arnold RG, Agarwal SK, Phelps P, et al. 1993. *Appl. Environ. Microbiol.* 59:2771–76
85. DiSpirito AA, Zahn JA, Graham DW, Kim HJ, Larive CK, et al. 1998. *J. Bacteriol.* 180:3606–13
86. Téllez CM, Gaus KP, Graham DW, Arnold RG, Guzman RZ. 1998. *Appl. Environ. Microbiol.* 64:1115–22
87. Kim HJ, Galeva N, Larive CK, Alterman M, Graham DW. 2005. *Biochemistry* 44:5140–48
88. Hakemian AS, Tinberg CE, Kondapalli KC, Telser J, Hoffman BM, et al. 2005. *J. Am. Chem. Soc.* 127:17142–43
89. Choi DW, Antholine WE, Do YS, Semrau JD, Kisting CJ, et al. 2005. *Microbiology* 151:3417–26
90. Choi DW, Zea CJ, Do YS, Semrau JD, Antholine WE, et al. 2006. *Biochemistry* 45:1442–53

Annual Review of Biochemistry

Volume 76, 2007

Contents

Mitochondrial Theme

Indexes

Errata

An online log of corrections to *Annual Review of Biochemistry* chapters (if any, 1997 to the present) may be found at http://biochem.annualreviews.org/errata.shtml